Query Details Back to Main Page

1. **Please confirm if the author names are presented accurately and in the correct sequence (given name, middle name/initial, family name). Author 1 Given name: [Maria Laura] Last name [Costantino]. Also, kindly confirm the details in the metadata are correct.**

   I confirm that the names are correct.

2. **Please check and confirm the equation link 'Eq. 5' in Fig. 1 caption.**

   The equation link should be corrected as 'Eq. 1'

Shear-Induced Encapsulation into Red Blood Cells: A New Microfluidic Approach to Drug Delivery

Monica Piergiovanni, [1]✉

Phone +390223994317
Email monica.piergiovanni@polimi.it

Giustina Casagrande, [1]

Francesca Taverna, [2]

Ilaria Corridori, [1]

Marta Frigerio, [1]

Elena Bianchi, [1]

Flavio Arienti, [2]

Arabella Mazzocchi, [2]

Gabriele Dubini, [1]

Maria Laura Costantino, [1]

[1] LaBS (Laboratory of Biological Structure mechanics), Department of Chemistry, Materials and Chemical Engineering “Giulio Natta”, Politecnico di Milano, Piazza Leonardo da Vinci, 32, 20133 Milan, Italy

[2] Service of Immunohematology and Transfusion Medicine, Fondazione IRCCS Istituto Nazionale Tumori, Milan, Italy

Received: 27 May 2019 / Accepted: 9 August 2019

Abstract

Encapsulating molecules into red blood cells (RBCs) is a challenging topic for drug delivery in clinical practice, allowing to prolong the residence time in the body and to avoid toxic residuals. Fluidic shear stress is able to temporary open the membrane pores of RBCs, thus allowing for the diffusion of a drug in solution with the cells. In this paper, both a computational and an experimental approach were used to investigate the mechanism of shear-induced encapsulation in a microchannel. By means of a computational fluid dynamic model of a cell suspension, it was possible to calculate an encapsulation index that accounts for the effective shear acting on the cells, their distribution in the cross section of the microchannel and their velocity. The computational model was then validated with micro-PIV measurements on a RBCs suspension. Finally, experimental tests with a microfluidic channel showed that, by choosing the proper concentration and fluid flow rate, it is possible to successfully encapsulate a test molecule (FITC-Dextran, 40 kDa) into human RBCs. Cytofluorimetric analysis and confocal microscopy were used to assess the RBCs physiological shape preservation and confirm the presence of fluorescent molecules inside the cells.

AQ1

Keywords

Micro-particle image velocimetry
Computational fluid dynamic
Two-phase mixture model
Erythrocytes
Drug carrier
Microdevice
Micro-hemodynamics

Associate Editor Umberto Morbiducci oversaw the review of this article.

Electronic supplementary material

The online version of this article (https://doi.org/10.1007/s10439-019-02342-w) contains supplementary material, which is available to authorized users.

Introduction

The delivery of drugs through the vascular system is a primary biomedical challenge. The use of complex drugs, together with the need to reach every site of the body, pushes the researchers towards the development of new carriers to promote specificity, effectiveness and safety of the delivery process. Among the cellular carriers, red blood cells (RBCs) have many advantages18,21: high volume and surface are available for the drug encapsulation due to the peculiar biconcave and a-nucleated shape of the cell. Moreover, RBCs have a long life cycle, thus allowing for a long permanence in the circulation flow, from where they can reach every district of the body. Finally, there are no toxic residuals in the body after the drug release and the carrier destruction. On the other hand,15 RBCs are quite difficult to manipulate, since they react to external stimuli by changing their morphology and the mechanical properties of their membrane. Moreover, a standardization of the drug encapsulation process remains a challenge, due to the different features of cells coming from various donors.

A number of drugs and various compounds (tracers, nanoparticles, *etc*.) are known to be effectively coupled with RBCs3–8,10,11,13,14,16,17,19,20,22–26,28 and different encapsulation techniques have been developed. The main mechanisms include loading the drug into the RBCs or coupling the molecule onto the surface of the cell *via* protein adhesion.27

Briefly, three methods are successfully used to entrap compounds into RBCs:

- Cell-penetrating peptides9 (CPP) are coupled to the chosen molecule and can successfully deliver it inside the RBCs through protein transduction;
- Electroporation1,4,6–13,19,20,22,27 induces pore opening by applying a high voltage across the RBCs membrane for a short time;
- Osmotic-based methods, which can be divided in hypotonic swelling1,4,6–8,10,11,13,19,22 and hypotonic dyalisis.2 By suspending the RBCs in a hypotonic solution, the osmotic pressure starts to push fluid inside the cells. Their membrane is thus stretched, temporary opening its porosity and allowing for molecule diffusion. A hypertonic solution is finally used to bring the RBCs back to their physiological condition.

Previous work performed in our laboratory5 proved that fluid shear stresses are able to temporary open the pores naturally present in RBCs membrane and allow for the diffusion of a molecule from the solution to the RBC cytoplasmic fluid. The exploitation of the microfluidic environment, where the viscous phenomena predominate, due to the high ratio between the internal channel surface and the volume of fluid, can lead to a fine control of the fluid solicitations acting on the cells membrane.

From a biomechanical point of view, mechanical stresses are reported to potentially induce haemolysis. Various indexes and models are used in the literature to find a threshold that accurately evaluates this phenomenon. The most widespread model was developed by Tillman,28 the first one to propose that the combined effect of force and exposure time was actually responsible for the RBCs death. Other models of mechanical haemolysis were developed in the years, a brief summary can be found in the S1 Supplementary Materials. Interestingly, none of these models actually indicates a sharp threshold, but rather a zone where the haemolysis risk is high. This is due to various biological and experimental conditions—detection method for the free haemoglobin, characteristic dimension of the setup, materials—but also to some properties that are specific of RBCs. In fact, the RBCs membrane is rather deformable and, until a certain extent, it can sustain deformations and recover its original shape and characteristics, thus creating a set of conditions that are commonly defined as sub-haemolytic.

In this work, a novel method for the drug encapsulation in RBCs is proposed. By optimizing geometrical and fluid dynamic parameters, it will be possible to induce a temporary pore opening without mechanically disrupting the cells, thus allowing for a diffusion of a test molecule. By optimizing the fluidic solicitation and the molecule concentration, it is possible to overcome some of the limitations of the constriction-induced intracellular delivery,25 where the loading is achieved by flowing different kind of cells through a series of micro-constrictions, requiring high pressures and a much diluted cell suspension.

Computational fluid dynamics (CFD) models were useful tools to support the design of microfluidic devices, both to select the proper experimental conditions and support the interpretation of the experimental results. When dealing with a dilute suspension of particles, it is possible to use mixture models,16 lacking the description of the physics of each particle but giving an overall vision on how the system works.

The validation of the CFD results is usually performed experimentally, thorough measurement of pressures and/or velocity distribution on a representative setup. The use of μ-PIV (micro Particle Image Velocimetry), that measures velocity fields with order 1-μm spatial resolution,14 is here proposed. This method was also applied to blood suspensions, in order to investigate how the presence of RBCs modifies the flow in particular geometries.26

Finally, the shear-induced encapsulation mechanism was tested on a pool of blood samples from human donors in various device configurations with a fluorescent test molecule.

Materials and Methods

A number of methods were used to thoroughly investigate the working principle of shear-induced encapsulation of molecules into RBCS.

Experimental tests were performed on RBCs collected from healthy human donors (9 male and 3 female under the clinical trial number 161/15 at Istituto Nazionale dei Tumori—Milan, Italy) and processed in a representative geometry. FITC-dextran was used as a test molecule and the impact of several parameters variation was statistically investigated. Table 1 summarizes all experimental parameters used and their alphanumeric code used throughout the present paper.

Table 1

Summary of the experimental parameters and corresponding alphanumeric code (e.g. Mα30 refers to an encapsulation in a channel with a length of 58.5 mm, with a solution containing 1 mg/mL dextran at a flow rate of 30 μL/min).

Channel length (mm)	Dextran concentration (mg/mL)	Flow rate (μL/min)
10 (S)	1 (α)	5
58.5 (M)	2 (β)	15
87 (L)	4 (γ)	30
117 (LL)		40
		50

Encapsulation Efficacy: Computational Approach

Model Characteristics

A computational model was developed using COMSOL Multiphysics 4.2a (COMSOL Inc., Stockholm, Sweden) to study the fluid dynamics of a cell

suspension. The Mixture Model, Laminar Flow was used to evaluate the local volume fraction of dispersed phase (Φ_d), in order to estimate the shear stress on RBCs suspended in PBS. This model accounts for rigid, spherical particles ($d_{RBC} = 8\ \mu m$) immersed in a liquid, continuous phase. The effect of gravity, which is relevant when evaluating the cell deposition, was also included. More details can be found in the S2 Supplementary Materials. In this work, as straight microchannel with a characteristic dimension of 50 μm was reproduced. After a sensitivity analysis, a mesh of 6.9 M elements was used for all simulations.

Simulations

Flow rate ranging from 0.25 to 100 μL/min were simulated, with haematocrit ranging from 1 to 10%. Due to the high number of possible combinations, a representative set of simulations was performed, covering the maximum range of flow rates practically feasible and the maximum range of haematocrit compatible with the dilute hypothesis of the mixture model. Velocity profile, flow regimen (by computing the Reynolds number *Re*), pressure drop across the channel, shear rate and encapsulation index were evaluated and analysed to identify the range of feasible experimental conditions.

Encapsulation Index

A normalized encapsulation index (Eq. 1) was defined to evaluate the flow conditions mainly influencing the encapsulation:

$$I_{encap} = \frac{v \cdot \tau \cdot \emptyset}{v_{max} \cdot \tau_{max} \cdot \emptyset_{max}} \quad (1)$$

where v is the velocity, τ is the shear stress and Φ is the volume fraction of RBC; the subscript refers to the maximum value in a reference cross section for each configuration. This index was designed to evaluate the effect of the different variables on the encapsulation process and compare the outcomes of the various CFD simulations, in order to identify a set of optimal configurations. Due to the particulate nature of the suspension here modelled, the encapsulation index is useful to visualize the different effects of velocity and shear stress on the individual cells, based on the portion of the cross–section they are flowing through.

In Vitro Model Validation by Micro PIV Analyses

μ-PIV measurements were used for the validation of the CFD model.

Experimental Setup

The experimental setup was composed by a syringe pump (Harvard Apparatus PHD 2000, Massachusetts, US), a 1 mL glass syringe (Gastight Syringes, Hamilton Bonaduz AG, Switzerland) with a 18G needle connected with silicon tubing to a straight microchannel. Commercially available chips (Microfluidic ChipShop GmbH, Jena, Germany) were used for these proof of concept tests: PMMA microchannels with a square section of 50 × 50 μm and different lengths were chosen. The μ-PIV system (TSI Incorporated, Minneapolis, USA) is composed by an inverted microscope (Olympus IX71), a synchronised laser (Nd:YAG 532 nm) used to excite the tracer particles at two time points with a desired time interval and a standard PC. The emitted light from the particles was recorded by a camera (Power View 4 M) in double frame images, selected to obtain particles displacement of 6–12 pixels. Red fluorescent polystyrene particles (d_p = 1 μm, Thermo Fisher Scientific, Waltham, MA, USA) were dispersed in a RBC solution (Ht = 1 and 5%) with a ratio on 1:10 and used as tracers.

Methods

The μ-PIV system is based on an algorithm to correlate couples of images, acquired with a proper time lapse (Δt), to obtain a velocity field. By averaging several couples of images with an 'ensemble PIV', it is possible to increase accuracy and reliability of the velocity profile obtained, significantly reducing the error and noise caused by out-of-focus fluorescent particles.23 100 couples of images for each flow rate were acquired focusing in the middle of the channel. The optics had a magnification of × 10, corresponding to a calibration of 0.46 μm/pixel. A grid of rectangular interrogation areas (32 × 64 pixel, with a 50% overlapping in both directions) was built. Flow rates up to 50 μL/min were tested and the obtained velocity profiles were compared with those predicted by the CFD model in the same flow rate range.

Shear-Induced Encapsulation: Experimental Evaluation

Encapsulation Process

Blood was suspended in a 1:3 solution v/v of phosphate buffer saline (PBS—Sigma-Aldrich S.r.l., Milan, Italy) and centrifuged at 4000 rpm for 5 minutes to separate RBCs from plasma and other cells. After the supernatant removal, RBCs were re-suspended in PBS to obtain a final solution at 1% haematocrit. Finally, an adequate quantity of 40 kDa FITC-dextran (Sigma-Aldrich S.r.l., Milan, Italy) was added to obtain the desired molecule concentration. Experiments were performed with three different dextran concentrations of 1, 2, and 4 mg/mL.

The loading setup is the same one used for micro-PIV analyses. The imposed flow rate and the channels length were varied to study the effect of solicitation and time on the encapsulation process. Microchannels of different length were tested at the same flow rates. This protocol allowed us to compare samples processed at the same shear stress values but at varying exposure times, thus analysing the effect of the shear-induced solicitation both in terms of molecule encapsulation and of mechanical haemolysis. 100 μL of the processed suspension was collected for the following analysis, re-suspended in PBS and centrifuged again to remove exceeding dextran in solution, for a total of three rinses.

Flow Cytometer Analyses

Samples were analysed with a flow cytometer (BD FACSCalibur, BD Biosciences, Becton Dickinson Italia, Milan, Italy) to verify the fluorescence and the morphology of the processed cells. Flow activated cell sorting (FACS) is used in laboratory practice to measure specific features of single cells in a sample by analysing the side scatter (SSC) and the forward scatter (FSC) of a laser beam, as well as fluorescence. In particular, the FSC gives an indication of the cell size, while the SSC gives an indication of the cell complexity. When referring to RBCs, SSC refers to the morphology of the cell, identifying normal cells, with the physiological biconcave shape, from damaged one, called echinocytes or stomatocytes.5 Each measure was taken twice on a 20,000 cells sample. The fluorescence was evaluated taking the geometrical mean of the sample, calculated with Eq. (2), where x_i is the fluorescence of each cell and n is the total number of cells.

$$\mathrm{geo}_{\mathrm{mean}} = \frac{\log \sum x_i}{n} \qquad 2$$

To evaluate the process efficiency, the fluorescence was calculated with Eq. (3) by comparison with a non-treated sample, taken as control.

$$\mathrm{efficiency}\,[\%] = \frac{\mathrm{geo}_{\mathrm{mean}}^{\mathrm{sample}} - \mathrm{geo}_{\mathrm{mean}}^{\mathrm{control}}}{\mathrm{geo}_{\mathrm{mean}}^{\mathrm{sample}}} \cdot 100 \qquad 3$$

Confocal Microscopy

Confocal images (Fluoview FV10i, Olympus) were taken to verify the actual encapsulation of the fluorescent dextran into the cells. This method was crucial to prove that the molecule is effectively trapped inside the RBCs and not

attached to the membrane on the outside. A stack of 12 images ($\Delta z = 0.8\ \mu$m) was acquired to completely capture a single cell.

Statistical Analysis

A preliminary descriptive analysis of dependent and independent variable has been performed. Each flow cytometer analysis has been repeated twice, Pearson's correlation coefficient and Lin's concordance correlation coefficient have been used to verify the repeatability of the acquisition. The normality of the samples in groups defined by channel length, dextran concentration and fluorescence geometric mean was verified using Kolmogorov–Smirnov–Lilliefors tests, then T test was used to compare fluorescence geometric mean at different flow rate with respect to control. Finally, a linear multivariate regression was used to assess the effect of the main parameters on the encapsulation process. The geometric mean of fluorescence was chosen as dependent variable. In order to reduce the complexity of the multivariate regression model, a preliminary bivariate correlation analysis was performed on all patient-specific variables (see S3 Materials for more details on this step). Only variables with a bivariate correlation coefficient higher than 0.3, were included in the subsequent regression. The regression coefficient B and its standard error were used as a reference to investigate the effect of each parameter on the output geo_{mean}. The experimental and physiological parameters included in the analysis were:

- Experimental parameters: dextran concentration [DX], channel length, flow rate;
- Patient-specific parameters: gender, RBC density [1/μL], haemoglobin (HB) [g/dL], haematocrit [%], MCV (mean cellular volume) [fL], MCH (mean HB content in each cell) [pg/cell], MCHC (mean density of haemoglobin in each RBC) [g/dL], RDW (RBCs volume variability in the sample) [%], age.

To account for the physiological differences among blood from various donors, an infraclass correlation coefficient (ICC) was calculated (See S4 Supplementary Materials). All statistical analysis were performed with the software SPSS (IBM, Armonk, USA).

Results

Computational Approach

Fluid Dynamics

The flow regime predicted by the computational model in the channel is laminar ($Re = 0.1–20$) for all the tested conditions, with a linear pressure drop across the channel that never exceeds 550 kPa (all data are summarized in Supplementary Table 1).

As can be clearly seen from Fig. 1, the model predicts a deposition of RBCs, especially near the outlet of the channel, at a flow rate of 0.25 μL/min (Fig. 1d), but this effect completely disappears when the flow rate is higher than 10 μL/min (Fig. 1e). At a distance of 50 μm from the inlet, the fluid reaches steady conditions and the velocity profile shows the typical parabolic shape (Fig. 1c).

Figure 1

Results of the CFD model on a representative cross section for a simulation at 30 μL/min and Ht = 5%. Shear stress (a), encapsulation index (b) calculated with Eq. (5), velocity magnitude (c). Volume fraction of the dispersed phase for low flow rate (d, 0.25 μL/min) and high flow rate (e, 30 μL/min) on a flow section close to the outlet.

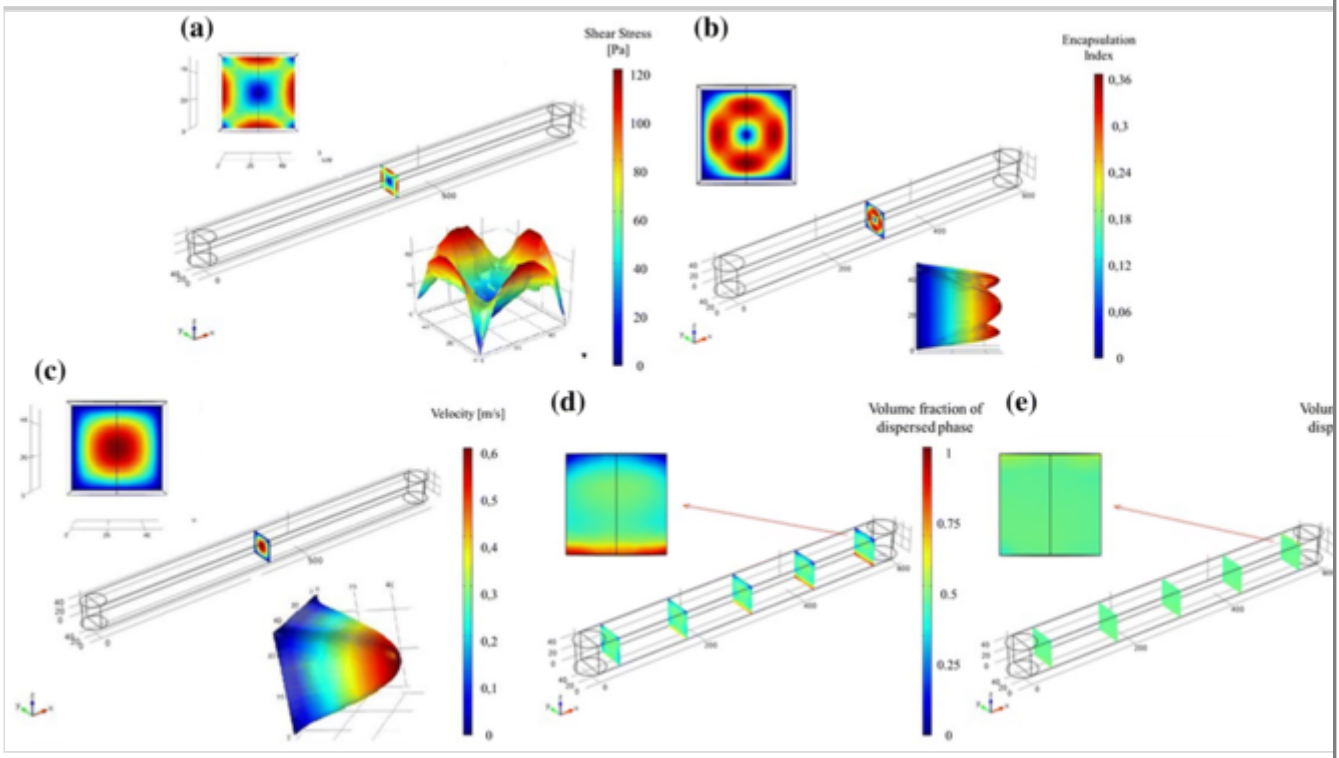

AQ2

Shear Rate and Encapsulation Index

The shear stress (τ) in the section of the channel is distributed as in Fig. 1a, while the velocity is represented in Fig. 1c. The encapsulation index I_{en} identifies the region of the channel, approximately 57.8% of the cross section,

where the three leading variables result in the optimum balance for promoting encapsulation. RBCs nearer to the wall, for instance, are subject to higher shear stress, but their velocity is rather low: in this situation, they undergo a high solicitation for a long time, thus the encapsulation index is close to 0. RBCs flowing in the centre, on the other hand, have a high velocity and a zero shear stress, thus the encapsulation cannot happen ($I_{en} = 0$). For the RBCs flowing at 0.6R, the velocity is 0.5 m/s, with a shear stress of 90 Pa; considering a uniform RBCs distribution, it is possible to have a I_{en} of 0.31.

By combining τ with velocity and RBC distribution in a representative cross-section, it is possible to identify a round crown region were I_{en} is higher than 0.2 (Fig. 1b), thus showing a region of optimal variable combination. This index is used to evaluate the effective shear stress (τ_{eff}) that acts on the RBCs, calculated averaging the shear stress acting on the cells flowing in this region.

It is widely known from the literature10 that RBCs tend to arrange themselves in a circular crown region almost coincident with the one found from the encapsulation index, leaving only a plasma layer near the walls, when blood flows in capillaries of 50–200 μm. In a dilute suspension, inertial forces become relevant for particle Reynolds number $Re_p > 1$ and both rigid spheres and deformable particles, undergo axial migration and experience the tubular pinch effect, reaching an equilibrium position of 0.6R, where R is the hydraulic radius of the micro channel. This zone corresponds to the crown region of the highest I_{en}, confirming that the majority of the cells can effectively flow in the region of optimal encapsulation conditions.

In Vitro Validation of the Computational Model

The velocity field observed by μ-PIV analyses has the typical parabolic shape, with maximum velocity in correspondence of the channel axis. For instance, for a flow rate of 30 μL/min and $Ht = 1\%$, the maximum velocity at the central axis is 0.3 m/s (Fig. 2, left panel). By comparing the μ-PIV average velocity profile with the one predicted by the CFD model (Fig. 2, right panel) the maximum error can be detected at the velocity peak, due to some limitations in the camera in capturing extremely high velocities. By looking at the velocities conditions in regions at high I_{en}, however, the computational results are confirmed by the experimental measurements.

Figure 2

On the left, colour map of micro-PIV velocity for a flow rate of 30 μL/min and $Ht = 1\%$. On the right, velocity comparison of the micro-PIV (solid line, data are shown as mean and SD on 100 image pairs) and CFD (dashed line) for the same

fluid dynamic conditions. I_{en} is also reported at varying length, same colour scale as Figure 1 is used.

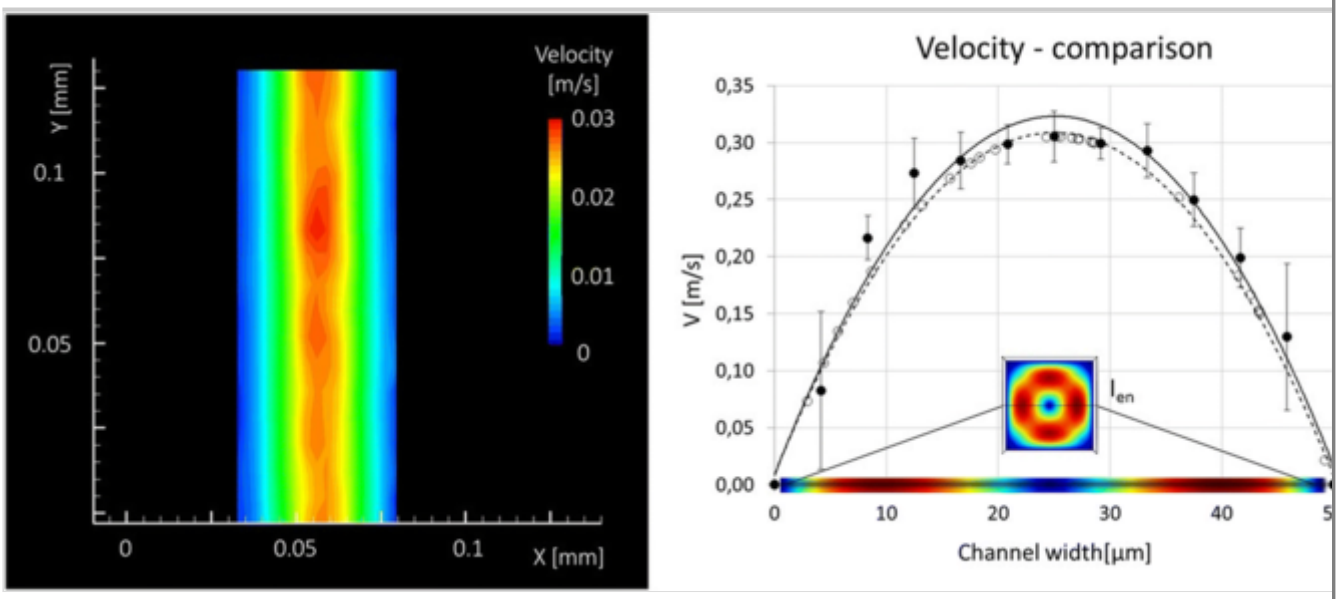

Experimental Encapsulation Tests

Flow Cytometer Analysis

In order to verify the absence of any alteration or damage to the cells, flow cytometer analysis were performed on all samples. Figure 3 bottom panel, shows that treated and control cells have similar cytograms.

Figure 3

Flow cytometer analyses of different encapsulation conditions, each dot corresponds to a single event (cell or debris). The cells remain mainly in the R1 portion of the diagram, associated with physiological RBC, with the classical biconcave shape. R2 and R3 zones contain echinocytes, altered RBCs that have a higher complexity due to a modified response to external stimuli. Top panel, high number of fragments, characterized by small dimensions can be seen in the red circle, showing the effect of channel length (a: Lβ15; b: LLβ5). Bottom panel, physiological cytograms corresponding to different flow rates (c: Mβ0, d: Mβ15, e: Mβ40).

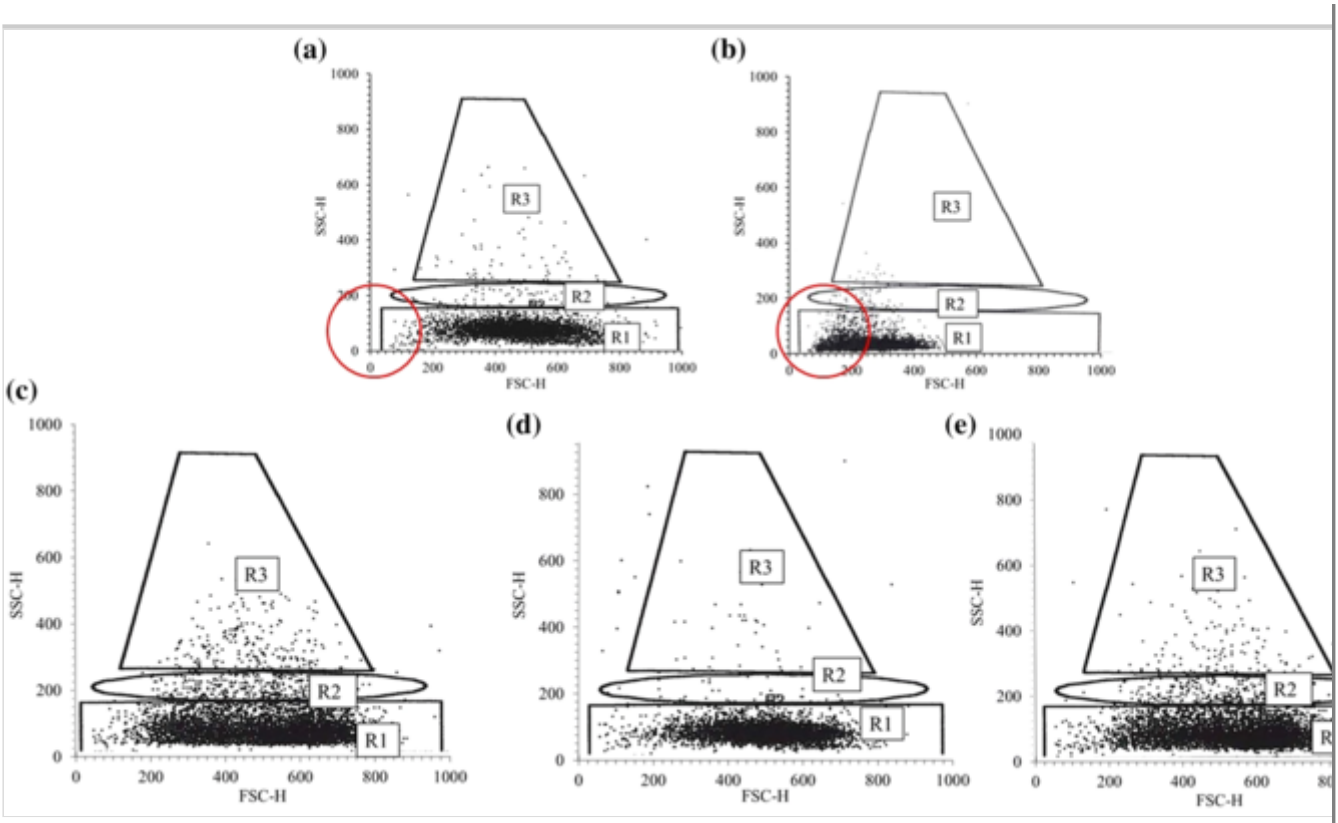

Flow cytometer analysis also allows evaluating the entity of the encapsulation in each experimental condition. Supplementary Figure 1S shows the increase in the sample fluorescence, induced by the presence of the encapsulated FITC-Dextran, with respect to the control sample for some representative tests. By means of cytometry analysis, it was also possible to measure the mechanical haemolysis on the processed sample at various conditions, indicated by a presence of RBCs fragments higher than 0.1% in the zone of low dimensions, marked with a red circle. In the longer microchannels, the exposure time was so high that it started to induce mechanical disruption of the cells even at the lower tested flow rates (5 and 15 μL/min).

Governing Parameters

The fluidic action on RBCs flowing in a micrometric channel is able to temporary open pores on the membrane, through which a test molecule, previously dispersed in the surrounding fluid, can diffuse. In every configuration tested, a significant increase in the fluorescence of the cells can be detected with respect to the control. Figure 4 reports the data related to the M channel (58.5 mm), where 0 μL/min represents the control, that is pure diffusion of FITC-Dextran in non-sheared RBCs.

Figure 4

Fluorescence intensity for encapsulation tests in the microchannels. Data are represented as mean, SD, minimum and maximum.

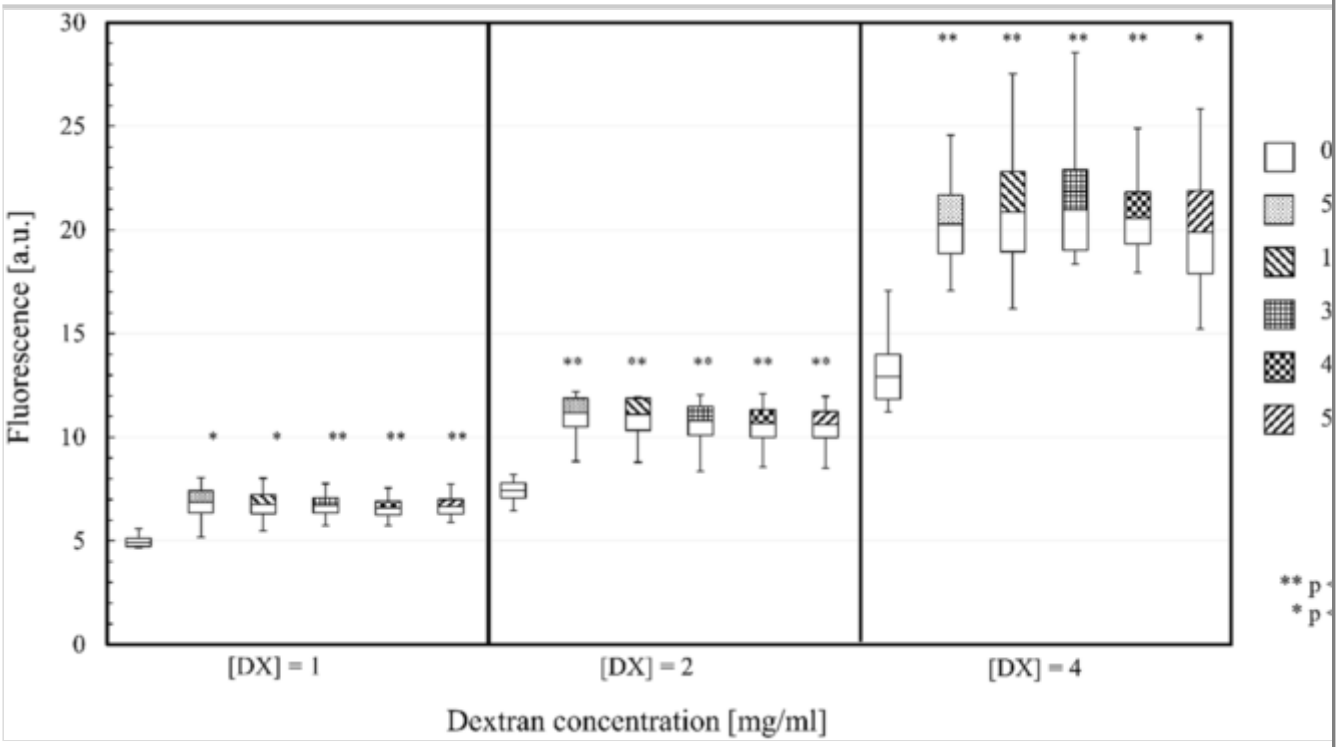

Dextran concentration greatly affects the encapsulation (Supplementary Figure 1S), due to the higher concentration gradient across the cell membrane. By varying the channel length, the encapsulation rate is rather affected. With the S channel a statistically significant encapsulation was reached only for Sγ15, Sγ30 and Sγ40 (p value < 0.05). An increase in the channel length, that in the present setup corresponds to an increase in exposure time, did not linearly correspond to an increase in encapsulation. Supplementary Figure 3S shows that an optimal encapsulation can be obtained with the channel M, corresponding to exposure times of 0.15-1.5 s. A short channel cannot offer a sufficiently high exposure time to have high encapsulation, while a longer channel is actually starting to produce haemolysis. This phenomenon is confirmed by looking at the cytograms relative to tests performed with longer microchannel (Figs. 3a and 3b), a shift of the signal in the left bottom corner indicates a massive presence of fragments. This effect is much more evident in the LL channel, indicating that the combination of fluidic shear and exposure time overcame the mechanical haemolytic threshold.28

The entity of the mechanical solicitation whose the RBCs undergo can be better evaluated by plotting the applied τ_{eff} and the exposure time in a Tillman diagram (Fig. 5). The pair of values $\tau_{eff} - t$ should be positioned in the sub-haemolytic zone of the diagram (between the solid and dashed lines) to obtain an adequate poration without incurring permanent damage of the RBCs.

Figure 5

Comparison of the computational and experimental results with the Tilmann (solid line) and haemolysis (dashed line) thresholds.

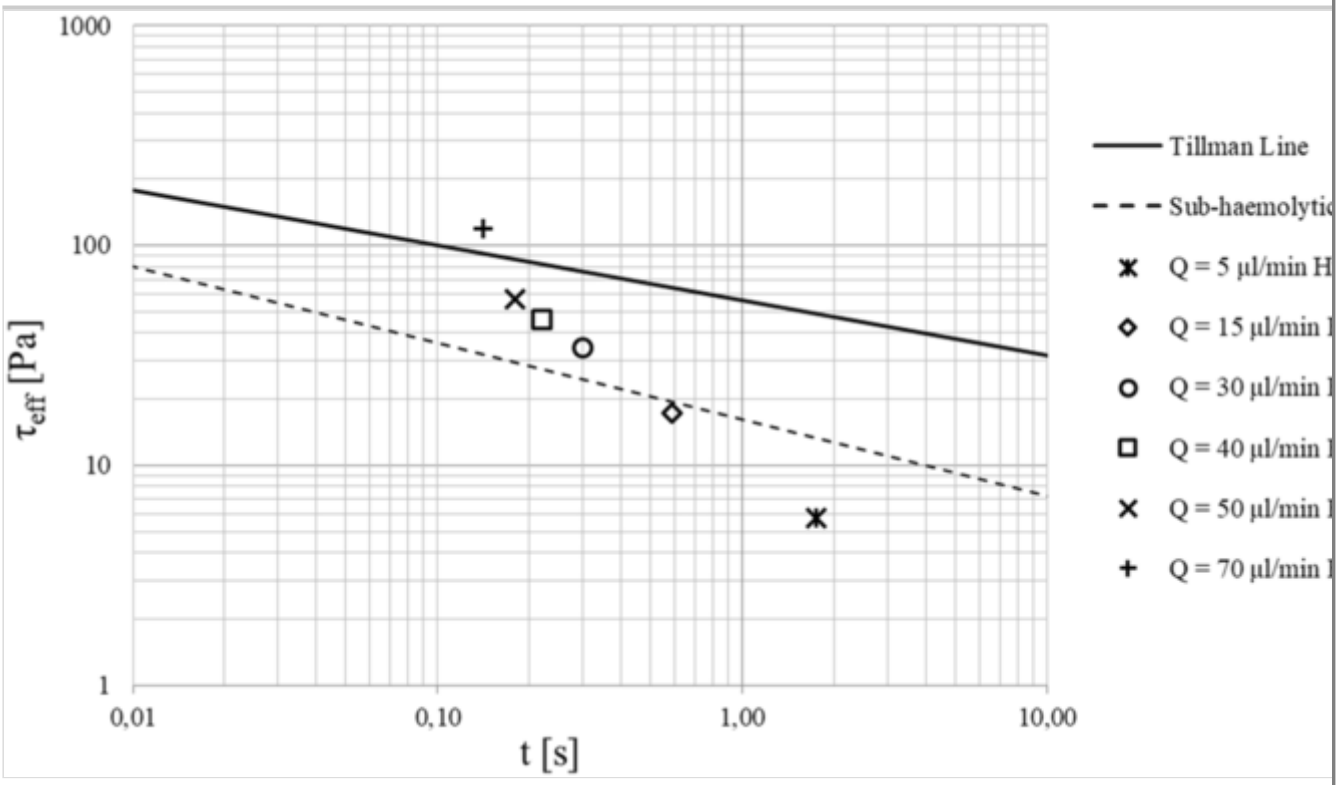

Confocal Microscopy

Samples from Mγ30 were also analysed through fluorescent confocal microscopy to confirm the presence of the FD40 molecule inside the cell (Fig. 6). It is possible to easily distinguish between RBCs with and without FITC dextran. Several optical planes were acquired on the same RBC, confirming that the molecule is trapped inside the cell.

Figure 6

Confocal microscopy. Left panel: fluorescent images of RBCs, numbers refer to top-bottom direction. Right panel: confocal images of FITC dextran encapsulated in a RBC from sample Mγ30. Scale bar is 10 μm and the z-distance between the images is 0.8 μm.

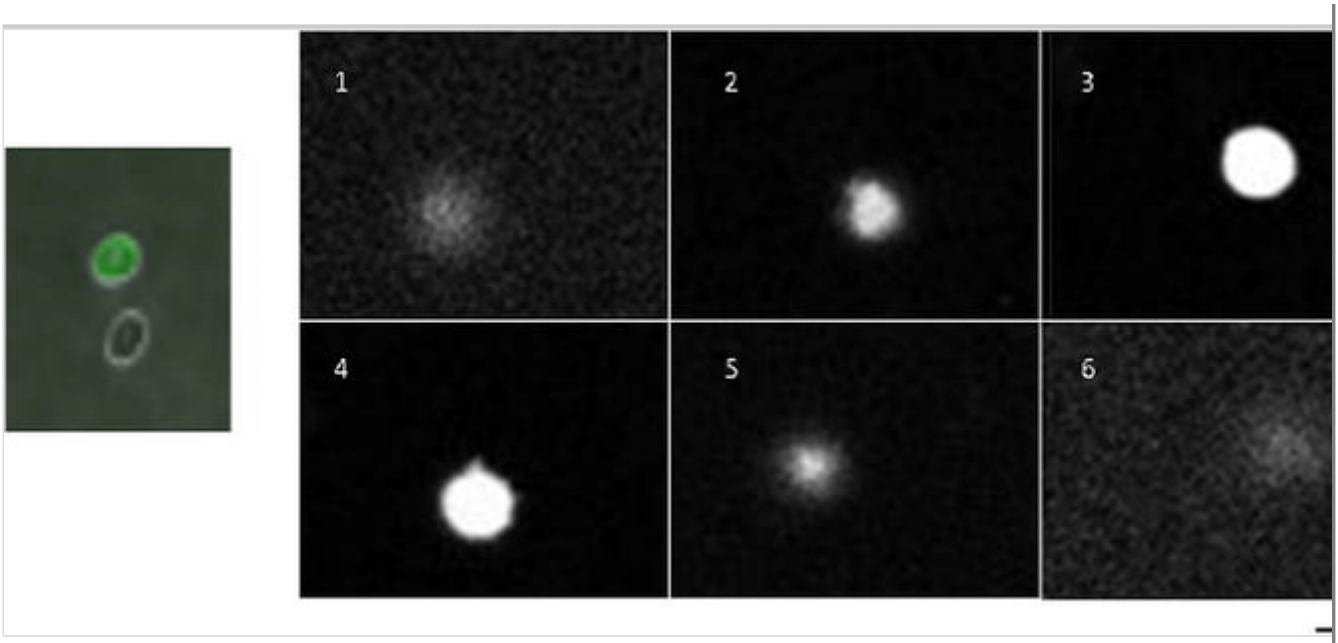

Multivariate Linear Regression

Multivariate linear regression model was used to estimate and weight the influence of different parameters on the geometric mean of fluorescence. According to the regression coefficients (Table 2), it can be asserted that the parameters mostly conditioning the geometric mean of the fluorescence are:

Table 2

Regression coefficient B and standard error of the multivariate linear regression for the estimation of the parameters effect on the geometric mean of the fluorescence.

Parameter	***B***	**Standard error**
Constant	21.101	14.608
Gender	*9.004*	*1.753*
MCV	*− 8.026*	*1.634*
[DX]	*3.102*	*0.171*
RDW	1.944	0.809
MCHC	0.898	0.430
Haemoglobin	0.559	0.710
Channel length	0.187	0.308
Flow rate	*0.048*	*0.013*
Results from all experiments were considered. In Italic the statistically significant parameters.		

- Concentration of dextran [DX];

- Gender;
- Erythrocytes Volume—Mean Cellular Volume (MCV): the RBCs of each donor have a different volume, thus a final solution with equal haematocrit (equal whole RBCs volume), will contain a different number of cells.
- Mean Corpuscolar Haemoglobin Concentration (MCHC): higher haemoglobin could hinder the encapsulation;
- Red blood cell distribution width (RDW): higher mean dimension of the cells indicates higher volume and thus more space for encapsulated probe molecule.

The effect of the donor accounts for about 19% of the total variability of the encapsulation process (see S5 Supplementary Materials).

Discussion

In this manuscript, the shear-induced encapsulation of a test molecule (FITC-dextran, 40 kDa) was obtained by mechanically stressing human RBCs by flowing them in a micrometric channel.

Preliminary studies performed in our lab, showed that a delicate balance between the shear stress applied on the RBC membrane and the molecular diffusion kinetics should be achieved. These two mechanisms, in fact, work in opposite directions: high values of flow rates are required to have shear stresses adequately high to induce poration, while sufficiently long exposure times (related to slower flow rates in our tested configurations) are necessary to allow the diffusion into RBCs.

By using the CFD model here described, it was possible to investigate the fluid dynamics of a RBCs suspension flowing in a microchannel in a wide range of working conditions. The high pressure-drop across the channel suggests that care should be taken in order to guarantee the seal of the setup and avoid loss of fluid. Nonetheless, the pressure range can still be managed with standard microfluidic equipment, without the need of metallic parts to strengthen the connections, one of the main limitation of similar encapsulation methods.25 The Mixture Model allows to visualise the distribution of the two phases in the channel, to identify eventual RBC deposition and then to set a correct range of flow rates where it can be assumed that the majority of the cells flowing in the channel are involved in the encapsulation process.

The use of a computational model gave useful indications and a more complete understanding of the process and the obtained results were experimentally validated using μPIV. The choice of this validation method is motivated by the fact that the literature reports several μPIV analysis on blood, providing accurate results both *in vitro* and *in vivo*, with haematocrit values up to 20% when using a confocal system, that allows for a 3D reconstruction of the velocity profile.11,19,22 Literature data, however, report flow rates that never exceed 1 μL/min, approximately 50 times lower than the experimental conditions here reported. Nonetheless, the validation here presented provided reliable results with high velocities (up to 0.3 m/s), at the cost of decreasing the haematocrit.

As described in the results section, the shear-induced method is primarily led by mechanical conditions, but many other parameters have a role in the outcome of the process. First of all, the concentration of the probe molecule is relevant, since it is the driving force of the diffusion through the membrane. Flow rate plays a role mainly related to the generation of fluid shear stresses on the cells, stresses that in the conditions here tested are always high enough to temporary open the membrane pores (Supplementary Figure 2S). Finally, the length of the channel is strictly related to the exposure time, since it relates to the total time of poration. For instance, using a short channel (10 mm) with all tested flow rates, the encapsulation rate was lower than with longer channels at the same flow rate, showing that the diffusion time of the molecule through the RBC membrane is longer than the exposure time.

The ability of the probe molecule to pass the cell membrane is also related with its steric diameter, 90 Å in the present study. Literature data6,25 show that larger molecules, up to 500 kDa, can be encapsulated into various types of cells by optimizing the condition for pore creation. Smaller molecules, on the other hand, could freely diffuse in and out of the RBCs also with a minimum membrane solicitation. The application with these compounds is usually coupled with a proper re-sealing method to secure stable encapsulation and avoid drug leakage.4

Other literature methods proved the importance of balancing the shear stress intensity and the exposure time. Prausnitz group,6 for instance, successfully developed a method of molecule uptake by prostate cancer cell lines, by applying a shear stress higher than 200 Pa for a short time, in the order of μs. The group of Jensen25 built on this approach to apply an instantaneous deformation in a constriction channel, squeezing the processed cells. Even if these approaches are efficient with many nucleated cells, they could present a high risk of inducing haemolysis when applied to RBCs.

From the statistical point of view, it is clear that some leading parameters are inherent to the donor. The gender seems to play a huge role in the encapsulation process, likely related to physiological differences.8 The RBCs mechanical properties are known to vary with the cell lifespan—younger RBCs are more deformable and can recovery much better after a deformation. Due to monthly blood loss, female blood contains more young and fewer old RBCs, suggesting a possible reason for a gender-specific response to sub-haemolytic shear stress (see Supplementary materials S4). The effect of the donor accounts for about 19% of the total variability of the encapsulation process. The biological viability among donors is an issue that will be furtherly investigated by increasing the number of donors and balancing the male/female samples.

Others methods specifically developed for drug loading into RBCs are described in literature: the application of lasers,17 electrical stress20 or chemical compounds7 makes these methods more difficult to use in clinical practice due to risk of chemical contamination of the sample or permanent damaging of the RBCs. The hypotonic dialysis method developed by Magnani *et al*.13 allows for a 30% encapsulation efficiency but still requires several steps of blood withdrawal and laboratory manipulation, leading to a final re-infusion into the patient that can happen hours after the first session.

Summarizing, our data show that this method allows for the entrapment of the molecule inside the cell with a very high efficacy. Depending on the working conditions, in particular on the flow rate and the dextran concentration, it is possible to successfully encapsulate drug in a high cell number, up to the 80% of all processed RBCs, without permanently changing the physiological morphology of the cell samples. Thanks to the many advantages offered by a microfluidic approach, the use of a single use device connected in-line with the patient, results an interesting way to have a faster and more secure process, minimizing the contamination with the external environment.

Acknowledgments

We thank Dr. Emanuela Iacchetti, Politecnico di Milano, for her essential help in the use of the confocal microscope and Dott. Mariangela Mazzi, Verona University, for helping setup the statistical analysis.

Conflict of interest M. Piergiovanni, G. Casagrande, E. Bianchi and M.L. Costantino filed a patent based on the results here presented (N. PCT/IB2018/060433—2018, December 21st).

Electronic supplementary material

Below is the link to the electronic supplementary material.

Supplementary material 1 (DOCX 473 kb)

References

1. Antonelli, A., C. Sfara, E. Manuali, I. J. Bruce, and M. Magnani. Encapsulation of superparamagnetic nanoparticles into red blood cells as new carriers of MRI contrast agents. *Nanomedicine* 6(2):211–223, 2011.

2. Banz, A., M. Cremel, A. Rembert, and Y. Godfrin. In situ targeting of dendritic cells by antigen-loaded red blood cells: a novel approach to cancer immunotherapy. *Vaccine* 28(17):2965–2972, 2010.

3. Biagiotti, S., M. F. Paoletti, A. Fraternale, L. Rossi, and M. Magnani. Drug delivery by red blood cells. *IUBMB Life* 63(8):621–631, 2011.

4. Bourgeaux, V., J. M. Lanao, B. E. Bax, and Y. Godfrin. Drug-loaded erythrocytes: on the road toward marketing approval. *Drug Des. Dev. Therapy* 10:665–676, 2016.

5. Casagrande, G., F. Arienti, A. Mazzocchi, F. Taverna, F. Ravagnani, and M. L. Costantino. Application of controlled shear stresses on the erythrocyte membrane as a new approach to promote molecule encapsulation. *Artif. Organs* 40(10):959–970, 2016.

6. Hallow, D. M., R. A. Seeger, P. P. Kamaev, G. R. Prado, M. C. LaPlaca, and M. R. Prausnitz. Shear-induced intracellular loading of cells with molecules by controlled microfluidics. *Biotechnol. Bioeng.* 99(4):846–854, 2008.

7. Harisa, G. I., M. F. Ibrahim, and F. K. Alanazi. Erythrocyte-mediated delivery of pravastatin: in vitro study of effect of hypotonic lysis on biochemical parameters and loading efficiency. *Arch. Pharm. Res.* 35(8):1431–1439, 2012.

8. Kameneva, M. V., M. J. Watach, and H. S. Borovetz. Gender difference in rheologic properties of blood and risk of cardiovascular diseases. *Clin. Hemorheol. Microcirc.* 21(3–4):357–363, 1999.

9. Kwon, Y. M., H. S. Chung, C. Moon, J. Yockman, Y. J. Park, S. D. Gitlin, A. E. David, and V. C. Yang. L-Asparaginase encapsulated intact erythrocytes for treatment of acute lymphoblastic leukemia (ALL). *J. Control Release* 139(3):182–189, 2009.

10. Lima, R., T. Ishikawa, Y. Imai, and T. Yamaguchi. Blood flow behaviour in microchannels: past, current and future trends. In: Single and 2-Phase Flows on Chemical and Biomedical Engineering, edited by R. Dias, R. Lima, A. A. Martins, and T. M. Mata. London: Bentham Books, 2012, pp. 513–547.

11. Lima, R., S. Wada, S. Tanaka, M. Takeda, T. Ishikawa, K. Tsubota, Y. Imai, and T. Yamaguchi. In vitro blood flow in a rectangular PDMS microchannel: experimental observations using a confocal micro-PIV system. *Biomed. Microdevices* 10(2):153–167, 2008.

12. Lizano, C., S. Sanz, J. Luque, and M. Pinilla. *In vitro* study of alcohol dehydrogenase and acetaldehyde dehydrogenase encapsulated into human erythrocytes by an electroporation procedure. *Biochim. Biophys. Acta* 1425(2):328–336, 1998.

13. Magnani, M., L. Rossi, M. D'ascenzo, I. Panzani, L. Bigi, and A. Zanella. Erythrocyte engineering for drug delivery and targeting. *Biotechnol. Appl. Biochem.* 28(1):1–6, 1998.

14. Meinhart, C. D., and J. G. Santiago. PIV measurement of a microchannel flow. *Exp. Fluids* 27:414–419, 1999.

15. Millan, C. G., M. L. S. Marinero, A. Z. Castaneda, and J. M. Lanao. Drug, enzyme and peptide delivery using erythrocytes as drug carrier. *J. Control Release* 95(1):27–49, 2004.

16. Mueller, S., E. W. Llewellin, and H. M. Mader. The rheology of suspensions of solid particles. *Proc. R. Soc. A* 466:1201–1228, 2010.

17. Mulholland, S. E., S. Lee, D. J. McAuliffe, and A. G. Doukas. Cell Loading with laser-generated stress waves: the role of the stress gradient. *Pharm. Res.* 16(4):514–518, 1999.

18. Muzykantov, V. R. Drug delivery by red blood cells: vascular carriers designed by mother nature. *Expert Opin. Drug Deliv.* 7(4):403–427, 2010.

19. Nakano, A., Y. Sugii, M. Minamiyama, and H. Niimi. Measurement of red cell velocity in microvessels using particle image velocimetry (PIV). *Clin. Hemorheol. Microcirc.* 29(3–4):445–455, 2003.

20. Phez, E., C. Faurie, M. Golzio, J. Teissié, and M. P. Rols. New insights in the visualization of membrane permeabilization and DNA/membrane interaction of cells submitted to electric pulses. *Biochim. Biophys. Acta* 1724(3):248–254, 2005.

21. Pierigè, F., S. Serafini, L. Rossi, and M. Magnani. Cell-based drug delivery. *Adv. Drug Deliv. Rev.* 60(2):286–295, 2007.

22. Poelma, C., P. Vennemann, R. Lindken, and J. Westerweel. In vivo blood flow and wall shear stress measurements in the vitelline network. *Exp. Fluids* 45(4):703–713, 2008.

23. Santiago, J. G., S. T. Wereley, C. D. Meinhart, D. J. Beebe, and R. J. Adrian. A particle image velocimetry system for microfluidics. *Exp. Fluids* 25(4):316–319, 1998.

24. Sharei, A., R. Poceviciute, E. L. Jackson, N. Cho, S. Mao, G. C. Hartoularos, D. Y. Jang, S. Jhunjhunwala, A. Eyerman, T. Schoettle, R. Langer, and K. F. Jensen. Plasma membrane recovery kinetics of a microfluidic intracellular delivery platform. *Integr. Biol.* 6(4):470–475, 2014.

25. Sharei, A., J. Zoldan, A. Adamo, W. Y. Sim, N. Cho, E. Jackson, S. Mao, S. Schneider, M.-J. Han, A. Lytton-Jean, P. A. Basto, S. Jhunjhunwala, J. Lee, D. A. Heller, J. W. Kang, G. C. Hartoularos, K.-S. Kim, D. G. Anderson, R. Langer, and K. F. Jensen. A vector-free microfluidic platform for intracellular delivery. *Proc. Natl. Acad. Sci.* 110(6):2082–2087, 2013.

26. Sherwood, J. M., D. Holmes, E. Kaliviotis, and S. Balabani. Spatial distributions of red blood cells significantly alter local haemodynamics. *PLoS ONE* 9(6):e100473, 2014.

27. Shi, J., L. Kundrat, N. Pishesha, A. Bilate, C. Theile, T. Maruyama, S. K. Dougan, H. L. Ploegh, and H. F. Lodish. Engineered red blood cells as carriers for systemic delivery of a wide array of functional probes. *PNAS* 111(28):10131–10135, 2014.

28. Tillman, W., H. Reul, M. Herold, K.-H. Bruss, and J. van Gilse. In vitro wall shear measurements at aortic valve prostheses. *J. Biomech.* 17:263–279, 1984.